603956

COPY 2 of 3 COPIES

AIR FORCE INSTITUTE OF TECHNOLOGY

AIR UNIVERSITY
UNITED STATES AIR FORCE

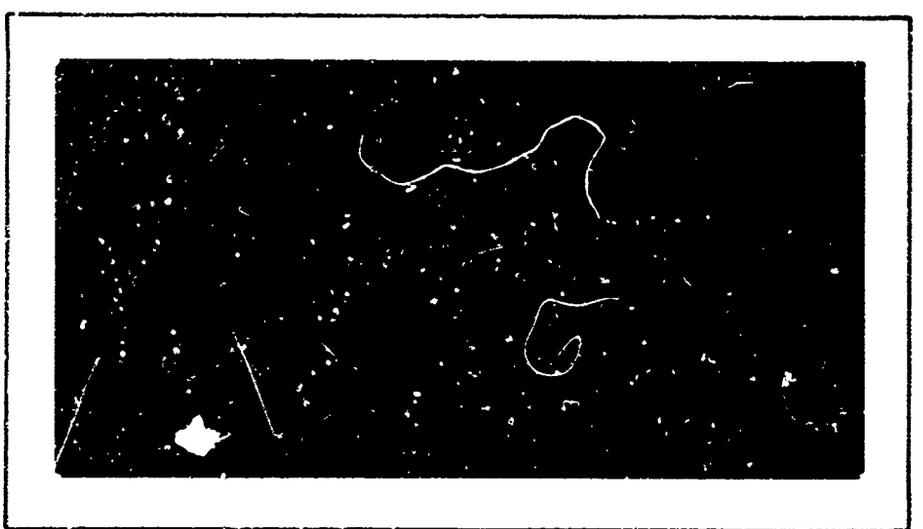

DDC
RELEASED
1964
DDC-IRA

SCHOOL OF ENGINEERING

WRIGHT-PATTERSON AIR FORCE BASE, OHIO

AF-WP-O-SEP 63 3M

Presented to the Faculty of the School of Engineering

The Air Force Institute of Technology

Air University

in Partial Fulfillment of the

Requirements for the

Master of Science Degree

in Electrical Engineering

UNCERTAINTY IN THE ESTIMATE OF POSITION AND VELOCITY ALONG A LUNAR TRAJECTORY USING INDIVIDUAL EARTH-MOON ANGULAR MEASUREMENTS IN A RECURSIVE NAVIGATION THEORY

THESIS

GGC/EE/64-9

PAUL J. ELLMER
Capt., USAF

DONALD R. HEFTY
Capt., USAF

Graduate Guidance and Control

June 1964

AF-WP-O-AUG 64 25

Preface

This report is our attempt to determine the feasibility of an earth-moon mission using a recursive navigation technique where only individual earth-moon fixes are used for navigational measurements. We believe that the report is organized in such a manner as to permit easy assimulation of the theories and techniques by the reader with some experience in lunar navigation studies. However, we do hope that the uninitiated can glean some informative meaning of the results and conclusions recorded. Since the introduction is the key to our pattern of development and sets forth the assumptions upon which this study is based, the reader should digest it before attempting the body of the report.

This study is by no means independent in the true sense of the word. As is obvious from the bibliography, it is based on the findings of several experts in the field of astronautical guidance. In particular, we would like to single out the work of Dr. Richard H. Battin of the M.I.T. Instrumentation Laboratory. Dr. Battin's well-formulated recursive navigation theory and matrix techniques are used exclusively in this study. It is safe to say that without them this study would have never been attempted. Also, we must acknowledge our faculty thesis advisor, Capt. Charles J. Januska, for suggesting this study and giving us the benefit of his insight into Dr. Battin's theory. Capt Januska's constant advice and encouragement made it possible for us to complete this study. Last,

but by no means least, we are grateful for the I.B.M. 7090 digital computer programming assistance of Mr. William R. Poole, a mathematician in the A.S.D. Digital Computation Division (WPAFB, Ohio). Without Mr. Poole's capable programming of our navigation equations and his interest and patience in making the many changes suggested as the study progressed, we could have never completed this study on time.

This investigation has been of great benefit to us in two distinct ways. First, we have become familiar with space navigation theories and gained an insight into the statistical theory upon which they are based. Secondly, we have gained invaluable experience in digital programming techniques.

Paul J. Ellmer

Donald R. Hefty

Contents

Contents

List of Figures

List of Tables

Abstract

The purpose of this study is to determine the feasibility of using a recursive navigation theory in which individual earth-moon angular measurements (fixes) are processed as they are made and combined with the current best estimate of position and velocity to produce an improved estimate. The recursive navigation techniques of Dr. Battin of the M.I.T. Instrumentation Laboratory are used. Estimates made with an earth-moon fix interval of 5 minutes or less are compared to estimates made with conventional earth-star, moon-star fixes of 15 minutes. Results show the earth-moon fix to be a feasible technique.

GGC/EE/64-9

UNCERTAINITY IN THE ESTIMATE OF POSITION AND VELOCITY ALONG A LUNAR TRAJECTORY USING INDIVIDUAL EARTH-MOON ANGULAR MEASUREMENTS IN A RECURSIVE NAVIGATION THEORY

I. Introduction

The design and development of self-contained lunar space navigation techniques are of paramount interest to many of the space scientists and astronautical engineers of today. The most critical factors in the design of such techniques are the accuracy and reliability of the spacecraft equipment needed to implement them. Since the navigation system is one of the most complex of the spacecraft subsystems, special attention has been given to reliability. Generally, this reliability is enhanced by the use of simple equipment concepts. Therefore, efforts to design new techniques, as well as modify present techniques, utilizing simpler equipment concepts is a continuous process. This study is concerned with the simplification of a proven concept of space navigation as applied to an earth-moon mission and is justified on the basis that a simplification of equipment can be obtained without sacrifice to accuracy.

Statement and Analysis of the Problem

A unique injection (launch)velocity imparted to an earth orbiting

vehicle at a specific point in space will result in an unique preplanned trajectory. As a result of injection velocity errors, however, the spacecraft will not follow this preplanned trajectory. Therefore, in order to determine the actual trajectory, navigational information must be obtained during the flight. A source of this navigational information in space is the observation of the angle between selected celestial bodies as seen from the spacecraft. It can be readily appreciated that an angular measurement between two celestial bodies is unique to only one point in space for any given time. Each angular measurement (navigational measurement, navigational fix, or simply, fix) need not determine the position and velocity of the spacecraft; the information from a series of individual fixes taken over a period of time may be combined as a recursive operation in which individual measurements are processed as they are made and combined with the current best estimate to produce an improved estimate. Theoretically, six such fixes would suffice to determine the position and velocity of the spacecraft. However, due to the inherent inaccuracies of the onboard angular measurement devices (an optical sextant in this study), statistical methods based on the known statistical behavior of these devices are necessary to ascertain the uncertainty (r.m.s. error) in the position and velocity estimate obtained.

The recursive navigation theory of Dr. Richard H. Battin of the M.I.T. Instrumentation Laboratory is used in this study

(Ref 3:303-340). This theory involves the formulation of an optimum linear estimate as a recursive operation in which the best estimate of position and velocity obtained by the best choice of navigational fix is combined with newly acquired information to produce an improved estimate. The derivation of the optimum linear operation is based on the application of a simple least-squares estimation technique.

The Problem. This study is concerned with the determination of the uncertainties in the estimates of position and velocity along a lunar trajectory using individual earth-moon angular measurements in a recursive navigation theory. The lunar trajectory in this study is defined as an elliptical path from a parking orbit about the earth to a point near the moon's sphere of influence (see Appendix A).

In previous studies made with the recursive navigation theory outlined, navigational measurements were made along the spacecraft's trajectory using various star-planet combinations. At each pre-planned measurement time, the particular star and planet (in a lunar trajectory study, several prominent stars and the planets, earth and moons are usually considered) contributing the least uncertainty in the estimate of position and velocity is selected. The analysis of the studies using this method, referred to as Fix 2 in this study, shows that acceptable accuracy was obtained (Ref 2:35-36).

In this study the fix at each preplanned point in time along the spacecraft's trajectory was restricted to the measurement of

the angle between the earth and moon only. This method is referred to as Fix 1 in this study. At first glance, this restriction seems to be unworthy of investigation because, given the same fix times for Fix 1 and Fix 2, it is obvious that Fix 2 is superior to Fix 1. However, considering smaller time intervals between the measurements of Fix 1, the situation takes on a new prospective. In Dr. Battin's studies, Fix 2 (Ref 2:28) was restricted to time intervals of no less than 15 minutes because of the time required to reposition the optical sextant to the next star-planet fix. In Fix 1, since the sextant is measuring only the earth-moon angle, no complex positioning arrangement need be implemented. Since the earth and moon is continuously monitored, fixes can be taken at much smaller time intervals. This allows more measurements to be made over a given span of time and increases the accuracy of the estimate of position and velocity at the end of that span.

Time intervals as small as 30 seconds were considered practical for Fix 1, since the only time restriction of any consequence was considered the processing time of the spacecraft's onboard digital computer. Therefore, in essence, this study is an investigation of using Fix 1 along a lunar trajectory at time intervals less than 15 minutes in a recursive navigation theory to determine whether or not it will give results comparable to Fix 2 at a time interval of 15 minutes.

Pattern of Development. The following sections attempt to outline the recursive navigation theory and show how it is applied to Fix 1 and Fix 2 to obtain the uncertainties in the estimate of position

and velocity along a lunar trajectory.

Section II contains a brief outline of the nature of the single observation fix and the linearized trajectory equations which are used in the recursive navigation theory. This section is supplemented by Appendixes A, B, and C. Appendix A describes the basic considerations in planning a lunar trajectory. The navigational fix equations are presented in Appendix B, while Appendix C presents the parameters of the lunar trajectory used in this study and states the equations which represent the deviations in position and velocity along the reference trajectory.

Section III gives some basic statistical considerations for the navigation theory and outlines the equations which define the uncertainties in the estimate of position and velocity at any point in time along the spacecraft's trajectory. Appendix D supplements Section III by presenting the assumed initial errors at injection of the spacecraft into its lunar trajectory and the assumed error of the optical sextant considered.

The results of Section IV graphically portray the comparison between Fix 1 and Fix 2 for different time intervals along the trajectory. In addition to this comparison, other factors observed which relate to the uncertainty in the position and velocity estimate using Fix 1 are presented. These factors are:

1. The effect of the inclination between the plane of the spacecraft's reference (preplanned) trajectory and the orbital plane of the moon.

2. The effect of the assumed r.m.s. error of the onboard optical sextant.

3. The effect of including in Fix 1 the apparent angular diameter measurements of the earth and moon.

The conclusions of Section V discuss the results obtained using Fix 1 and their meaning in terms of the compatability with uncertainties in position and velocity using Fix 2. Possible extensions to this study are outlined in the recommendations of Section VI.

Assumptions. The solution of this problem was based on the following assumptions:

1. The spacecraft's motion is adequately described in a single inverse squared gravity field (earth). This assumption is discussed in more detail in Appendix A.

2. The location of stars was arbitrarily selected along the six axes of the space coordinate system (Appendix C) and at an infinite distance. This assumption is valid because the direction of the stars, corrected for aberration and parallax for the period of a lunar mission, are, for all practical purposes, unvarying regardless of vehicle position. Also, aboard the spacecraft the stars are unobscured and appear as point sources of light.

3. The features of the moon can be readily observed from a spacecraft and the terrain features on earth will also be observable from the spacecraft despite some degradation due to atmospheric effects. Therefore, the use of an onboard optical sextant suggests itself as one possible technique for making angular measurements.

4. The only equipment inaccuracies considered are in the optical sextant of the spacecraft's navigational system. In addition, the optical sextant is assumed to have a known random and independent error. Section III and Appendix D outline this assumption in more detail.

5. The deviations from the reference trajectory are small enough to allow the use of linearized techniques. This assumption is justified on the premise that only small deviations can be tolerated on this type of mission without making corrective techniques impractical because of the limited fuel capacity of the vehicle.

6. Initial position and velocity errors can be predicted within a certain tolerance. The prediction used in this study is outlined in Appendix D.

7. Only the outbound portion of a circumlunar mission between an earth parking orbit and the moon's sphere of influence was considered. This assumption is discussed further in Appendix A.

8. Finally, the onboard computer is capable of storing all pertinent constants and computing the navigation and guidance problem in the time allowed.

Notational Conventions

The notational conventions used in this study are those used by Dr. Battin (Ref 2:2). Most of the equations in this report

are three-and six-dimensional vector equations and are denoted by a capital letter such as A, K, T, etc. A column matrix of any dimension is represented by a lower case underscored letter such as $\underline{a}$. A vector transpose is denoted $\underline{a}^T$ and the scalar or dot product of two vectors $\underline{a}$ and $\underline{b}$ is written $\underline{a}^T\underline{b}$. An overscorce denotes the average value, therefore, $\bar{\underline{a}}$ is the average value of the vector $\underline{a}$.

II. A Linearized Navigational Theory

A single angular measurement made at a known instant of time is sufficient to fix the position of the spacecraft in one coordinate. Succeeding measurements combined with updated position information from preceding measurements suffice to accurately determine the spacecraft's position and velocity (Ref 2:3-4). The practicality of this method is based on the fact that vehicle dynamics are governed by known laws and the assumption that deviations from a preplanned trajectory are kept small enough to permit linearization of the problem. A discussion of the nature of the single angle fix and of the linearized trajectory equations which constitute this method is outlined in this section.

A Single Observation Fix

As stated, a single measurement serves to fix the position of the spacecraft in one coordinate, if a linearized theory is assumed (Ref 8:12). It is shown in Appendix B that the deviation in position, $\delta \underline{r}_n$, of the spacecraft from the reference path is related to the deviation in angular measurement, δA_n, by

$$\delta A_n = \underline{h}_n^T \delta \underline{r}_n \tag{1}$$

if the observation is made at a known instant of time, t_n. The vector $\underline{h}_n$ is a function of the geometry of the celestial objects measured and the type of measurement.

Because of the inherent dynamic coupling of position and velocity, the result at a later time, t_{n+1}, of a measurement made at t_n does not lend itself to a simple geometric interpretation. However, to provide a geometric description it is convenient to define the state of the vehicle dynamics at t_n by the six dimensional deviation vector

$$\delta \underline{x}_n \quad \begin{bmatrix} \delta \underline{r}_n \\ \delta \underline{v}_n \end{bmatrix} \tag{2}$$

where $\delta \underline{v}_n$ is the deviation in velocity. The relationship between $\delta \underline{x}_{n+1}$ and $\delta \underline{x}_n$ is simply

$$\delta \underline{x}_{n+1} = T_{n+1,n} \delta \underline{x}_n \tag{3}$$

where $T_{n+1,n}$ is referred to as the "state transition matrix" and is defined later by Eq (19).

Equation (1) may be written in terms of $\delta \underline{x}_n$ as

$$\delta A_n = h_n^T K^T \delta \underline{x}_n \tag{4}$$

where the rectangular K matrix is defined by

$$K = \begin{bmatrix} I \\ O \end{bmatrix}_{6X3} \tag{5}$$

By combining Eqs. (3) and (4), we have

$$\delta A_n = \underline{h}_n^T K^T T_{n+1,n}^{-1} \delta \underline{x}_{n+1} \tag{6}$$

Six observations made at different times would provide a set of six equations of the form of Eq. (6). If no two of the component directions were parallel and the measuring device used

to obtain δA_n was perfect, then the deviation vector could be accurately computed.

Matrix Solution of the Trajectory Equations

A certain collection of so-called "perturbation" matrices are basic to the solution of the linearized trajectory problem. The following shows how these matrices may be obtained as solutions of the linearized differential equations.

Let $\underline{r}_s(t)$ and $\underline{v}_s(t)$ denote the position and velocity of the spacecraft in an earth centered inertial coordinate system, and let $\underline{g}(\underline{r}_s,t)$ denote the gravitational acceleration. Then

$$\frac{d\underline{r}_s}{dt} = \underline{v}_s \quad , \quad \frac{d\underline{v}_s}{dt} = \underline{g}(\underline{r}_s,t) \tag{7}$$

are the basic free fall equations of motion.

Let $\underline{r}_o(t)$ and $\underline{v}_o(t)$ represent the position and velocity associated with the reference trajectory at time t and define

$$\underline{r}(t) = \underline{r}_s(t) - \underline{r}_o(t) \ , \quad \underline{v}(t) = \underline{v}_s(t) - \underline{v}_o(t) \tag{8}$$

Then, the deviations $\delta \underline{r}$ and $\delta \underline{v}$ may be approximately related by the linearized differential equations

$$\frac{d(\delta \underline{r})}{dt} = \delta \underline{v} \quad , \quad \frac{d(\delta \underline{v})}{dt} = G(\underline{r}_o, t)\delta \underline{r} \tag{9}$$

where $G(\underline{r}_o,t)$ is a 3 dimensional matrix whose elements are the partial derivatives of the components of $\underline{g}(\underline{r}_o,t)$ with respect to the components of $\underline{r}_o$ (Ref 15:62).

A fundamental set of solutions of Eqs (9) has been developed (Ref 3:210). Let t_L and t_A be the time of launch and arrival, respectively. Then define the 3 dimensional matrices R(t), R(t)*, V(t) and V(t)* as the solutions of the matrix differential equations

$$\frac{dR(t)}{dt} = V(t) \qquad \frac{dR(t)^*}{dt} = V(t)^* \qquad (10)$$

$$\frac{dV(t)}{dt} = GR(t) \qquad \frac{dV(t)^*}{dt} = GR(t)^*$$

which satisfy the initial conditions

$$R(t_L) = 0 \qquad R(t_A)^* = 0 \qquad (11)$$

$$V(t_L) = I \qquad V(t_A)^* = I$$

If we now write

$$\delta \underline{r}_n = R_n \underline{c} + R_n^* \underline{c}^* \qquad (12)$$

$$\delta \underline{v}_n = V_n \underline{c} + R_n^* \underline{c}^* \qquad (13)$$

where $\delta \underline{r}_n = \delta \underline{r}(t_n)$, $R_n = R(t_n)$, etc., and $\underline{c}$ and $\underline{c}^*$ are arbitrary constant vectors, it follows that these equations satisfy the linearized differential equations (9). They also contain precisely the required number of unspecified constants to meet any valid set of initial or boundary conditions.

The elements of the R_n and V_n matrices represent deviations in position and velocity along the reference trajectory resulting from velocity deviations at launch. A similar meaning is given

to the R_n^* and V_n^* matrices as a result of deviations in velocity at the arrival point. A complete description of these perturbation matrices can be found in the literature (Ref 15:58-66).

There are a number of techniques for computing these perturbation matrices. Since this study deals with an elliptical trajectory, a simple and straight forward matrix technique formulated by Dr. Battin (Ref. 1:761-773) was used. This technique, which is modified for the special case of a spacecraft trajectory coplanar to the orbit of the moon, is outlined in Appendix C.

The State Transition Matrix

The state transition matrix was defined by Eq (3) and can be computed from a knowledge of the Eqs (12) and (13). First, $\underline{c}$ and $\underline{c}^*$ must be obtained as solutions of Eqs (12) and (13). After some simplification

$$\underline{c} = -L_n^{-1}(C_n^* \delta \underline{r}_n - \delta \underline{v}_n) \tag{14}$$

$$\underline{c}^* = -L_n^{*-1}(C_n \delta \underline{r}_n - \delta \underline{v}_n) \tag{15}$$

where

$$\begin{aligned} C_n &= V_n R_n^{-1} \\ C_n^* &= V_n^* R_n^{*-1} \\ L_n &= V_n - C_n^* R_n \\ L_n^* &= V_n^* - C_n R_n^* \end{aligned} \tag{16}$$

Thus, with $\underline{c}$ and $\underline{c}^*$ determined, the position and velocity deviations at any time t_n are given by Eqs (12) and (13).

In terms of the six dimensional deviation vector defined by Eq (2),

$$\delta \underline{x}_n = \begin{bmatrix} R_n & R_n^* \\ V_n & V_n^* \end{bmatrix} \begin{bmatrix} \underline{c} \\ \underline{c}^* \end{bmatrix} \tag{17}$$

A similar relationship can be written for $\delta \underline{x}_{n+1}$. Considering Eq (3) we have

$$\delta \underline{x}_{n+1} = \begin{bmatrix} R_{n+1} & R_n^*{}_{+1} \\ V_{n+1} & V_n^*{}_{+1} \end{bmatrix} \begin{bmatrix} R_n & R_n^* \\ V_n & V_n^* \end{bmatrix}^{-1} \delta \underline{x}_n \tag{18}$$

Using Eqs (16), we have

$$T_{n+1,n} = \begin{bmatrix} R_{n+1} & R_{n+1}^* \\ V_{n+1} & V_{n+1}^* \end{bmatrix} \begin{bmatrix} (C_n^{*-1} L_n)^{-1} & 0 \\ 0 & (C_n^{-1} L_n^*)^{-1} \end{bmatrix} \begin{bmatrix} -I\ C_n^{*-1} \\ -I\ C_n^{-1} \end{bmatrix} \tag{19}$$

Further simplification gives

$$T_{n+1,n} = \begin{bmatrix} R_{n+1} & R_{n+1}^* \\ V_{n+1} & V_{n+1}^* \end{bmatrix} \begin{bmatrix} (R_n - A_n^* V_n)^{-1} (A_n^* V_n - R_n)^{-1} A_n^* \\ (R_n^* - A_n V_n^*)^{-1} (A_n V_n^* - R_n^*)^{-1} A_n \end{bmatrix} \tag{20}$$

(Ref 3:305)

where

$$A_n = C_n^{-1} = R_n V_n^{-1}$$

$$A_n^* = C_n^{*-1} = R_n^* V_n^{*-1} \tag{21}$$

The form of Eq (20) was motivated by the values of $R(t_L)$ and $R^*(t_A)$. From Eqs (16) it follows that these two singular matrices would make the computation of $C(t_L)$ and $C(t_A)^*$ impossible. However, this difficulty is avoided by the use of Eq (20).

An interesting feature of the state transition matrix, which allows the checking of its computation, is that it is an example of a symplectic matrix (Ref 3:306) . An even-dimensional matrix, A, is said to be symplectic if

$$A^T J A = J \tag{22}$$

where

$$J = \begin{bmatrix} O & I \\ -I & O \end{bmatrix} \tag{23}$$

In addition, the absolute value of the determinate of a symplectic matrix is equal to unity. These features were used to check the computation of the state transition matrices computed in this study.

III. An Estimate of Position and Velocity Deviation

The previous section described a simple position and velocity determining technique which made no provision for the inherent errors common to all navigational measuring instruments. Usually it is necessary to discuss navigational accuracy on a probabilistic rather than absolute basis because of the inexact knowledge of the error coefficients of the various measuring devices in the system. Therefore, a statistical evaluation of the accuracy of the navigation process must be made. In this study only the optical measuring device was considered as a source of the uncertainty. Accurate estimates of position and velocity along a space trajectory can be obtained by applying the method of least squares to the system's errors. A linear least squares estimation procedure, where all statistical calculations are based on first and second order averages, is outlined in this section (Ref 2:4-6).

Statistical Parameters and Definitions

Berore discussion of the statistical parameters, it is necessary to define some terms

δA_n = the true deviation in the angle A_n from its reference value at t_n

$\delta \tilde{A}_n$ = the observed or measured deviation

$\delta \hat{A}_n$ = the estimated deviation

$\delta \hat{A}_n'$ = $\delta \hat{A}_n$ extrapolated from a previous estimate by the state transition matrix (T)

a_n = the error in the measurement of δA_n

$\underline{b}_n$ = the error in position estimate

$\underline{d}_n$ = the error in velocity estimate

Similar definitions can be applied to $\delta \underline{x}_n$, Eq (2).

From these definitions we have,

$$\delta \tilde{A}_n = \delta \hat{A}_n + a_n \tag{24}$$

In the subsequent analysis, a_n will be assumed to be a random ($\overline{a_n} = o$) and independent ($\overline{a_{n-1} a_n} = o$) variable. The application of the Central Limit Theorem indicates that the probability distribution function for the system error will be normally distributed (Ref 9:315). Furthermore, the standard deviation (σn) for the system error will be the root-sum-square combination of the standard deviation for the individual error coefficients. Therefore, in this study the variance of the optical measuring device can be computed by

$$\sigma n^2 = \overline{a_n^2} \tag{25}$$

In the next sub-section, an estimation procedure is discussed for determining an optimum linear estimate of $\delta \underline{x}_n$, denoted by $\delta \hat{\underline{x}}_n$. An integral part of this estimation technique is the correlation matrix of the measurement errors in the estimate. If we write

$$\delta \hat{\underline{x}}_n = \delta \underline{x}_n + \underline{e}_n \tag{26}$$

then

$$\underline{e}_n = \begin{bmatrix} \underline{b}_n \\ \underline{d}_n \end{bmatrix} \tag{27}$$

The correlation matrix of the measurement errors is thus defined by

$$E_n = \overline{\underline{e}_n \underline{e}_n^T} = \begin{bmatrix} \overline{\underline{b}_n \underline{b}_n^T} & \overline{\underline{b}_n \underline{d}_n^T} \\ \overline{\underline{d}_n \underline{b}_n^T} & \overline{\underline{d}_n \underline{d}_n^T} \end{bmatrix} = \begin{bmatrix} E_n^1 & E_n^2 \\ E_n^3 & E_n^4 \end{bmatrix} \quad (28)$$

where the traces of E_n^1 and E_n^4 are the mean-squared errors in the estimate of position and velocity, respectively or as it is used in this report, the uncertainties in position and velocity. Again from the definitions we have

$$\delta \hat{\underline{x}}_n' = T_{n,n-1} \delta \hat{\underline{x}}_{n-1} \quad (29)$$

In like manner, the extrapolated correlation matrix can be shown to be

$$E_n' = T_{n,n-1} E_{n-1} T_{n,n-1}^T \quad (29A)$$

Improving the Estimate

The development of an optimum linear estimate as a recursive operation in which the current best estimate is combined with newly acquired information to produce a better estimate was presented by R.E. Kalman (Ref 12) and completely formulated by R. H. Battin (Ref 2:16-18). This development assumes that an initial E_{n-1} (Appendix D) is known and that a single navigational measurement of the type described in Appendix B is made at time t_n. A linear estimate for the deviation vector $\delta \underline{x}_n$ is expressible as

$$\delta \hat{\underline{x}}_n = \delta \hat{\underline{x}}_n' + \underline{w}_n (\delta \tilde{A}_n - \delta \hat{A}_n') \quad (30)$$

where $\underline{w}_n$ is a weighting factor which will be chosen so as to minimize the mean-square error in the estimate. It can be

shown that the correlation matrix, E_n defined by Eq (28) may be expressed as a function of $\underline{w}_n$ as

$$E_n(\underline{w}_n) = (I - \underline{w}_n\underline{h}_n^T K^T)\, E_n'(I - K\underline{h}_n\underline{w}_n^T) + \underline{w}_n\underline{w}_n^T\overline{a_n^2} \tag{31}$$

In order to determine the optimum $\underline{w}_n$, the technique of variation calculus can be shown to yield

$$\delta\,\overline{e_n^2(\underline{w}_n)} = 2tr\left[-\delta\,\underline{w}_n\underline{h}_n^T K^T E_n'\,(I - K\underline{h}_n\underline{w}_n^T) + \underline{w}_n\underline{w}_n^T\overline{a_n^2}\right] \tag{32}$$

If $\delta\,\overline{e_n^2(\underline{w}_n)}$ is to vanish for all variations $\delta\,\underline{w}_n$, then it must follow that

$$c_n\underline{w}_n = E_n'\,K\underline{h}_n \tag{33}$$

where the scalar coefficient c_n is computed from

$$c_n = \underline{h}_n^T K^T E_n'\,K\underline{h}_n + \overline{a_n^2} \tag{34}$$

Having obtained the optimum $\underline{w}_n$, E_n may be written as

$$E_n = E_n' - c_n^{-1}(E_n'\,K\underline{h}_n)\,(E_n'\,K\underline{h}_n)^T \tag{35}$$

Equations (30) and (35) then serve as recursive relations to be used in obtaining improved estimates of position and velocity deviations at each of the measurement times selected along the spacecraft's trajectory.

IV. Results

The effects on position and velocity uncertainties by use of various navigation fix schemes, altering the inclination angle between the reference trajectory plane and the lunar plane, considering different values for the variance in the errors of the optical measuring device, and using different time intervals between each navigation fix is outlined in this chapter. Finally, a comparison between Fix 1, which uses only earth-moon angular measurements for input into the recursive navigation equations and Fix 2, which considers and selects the best of earth-star, moon-star, and earth-moon angular measurements is presented in the last section of this chapter.

Since only the outgoing elliptical portion of the lunar trajectory is considered in this study, the final position and velocity uncertainties as listed actually represent the initial uncertainties for the selenocentric hyperbolic portion of the lunar trajectory. A value of one statute mile (Ref 5:13) was selected as the desired maximum uncertainty in final position and 0.025 mph was chosen as the desired maximum uncertainty in final velocity. This desired final maximum velocity corresponds to approximately 0.001% of the velocity of the vehicle at that point (Ref 6:31; Ref 16:755). It was also desired to maintain the maximum position and velocity uncertainties during the flight within an order of magnitude of those found by Battin (Ref 2:35-36). To help indicate the general shapes of the

curves, the tables in this chapter also include values at the midcourse point, which for this study is considered that point corresponding to 25 hours of flight.

Effect of Navigation Measurements

The effect of using various navigation fix schemes on the uncertainties in position and velocity is presented in Fig. 1 and Table I. Fix 1 uses only earth-moon angular measurements for input into the recursive navigation equations; Fix 2 considers and selects the best of the earth-star, moon-star, and earth-moon angular measurements; Fix 3 considers and selects the best of the apparent diameter measurements of the earth and moon, and the earth-moon angular measurements; and Fix 4 considers and selects the best from all of the above measurements. For each fix, the best measurement is considered that measurement which results in the smallest value for uncertainty in position. The measurements are further discussed in Appendix B. The inclination angle between the lunar plane and the reference trajectory plane is 90^0 (Appendix A) and the time interval between each navigation fix is held constant at 30 minutes. As indicated in Fig. 1, the position and velocity uncertainty curves each use different values for the variance in the errors of the optical measuring device.

The position uncertainty curve for Fix 3 exhibits unexpected results which have not been explained, although the pertinent equations and computer program have been checked for possible errors.

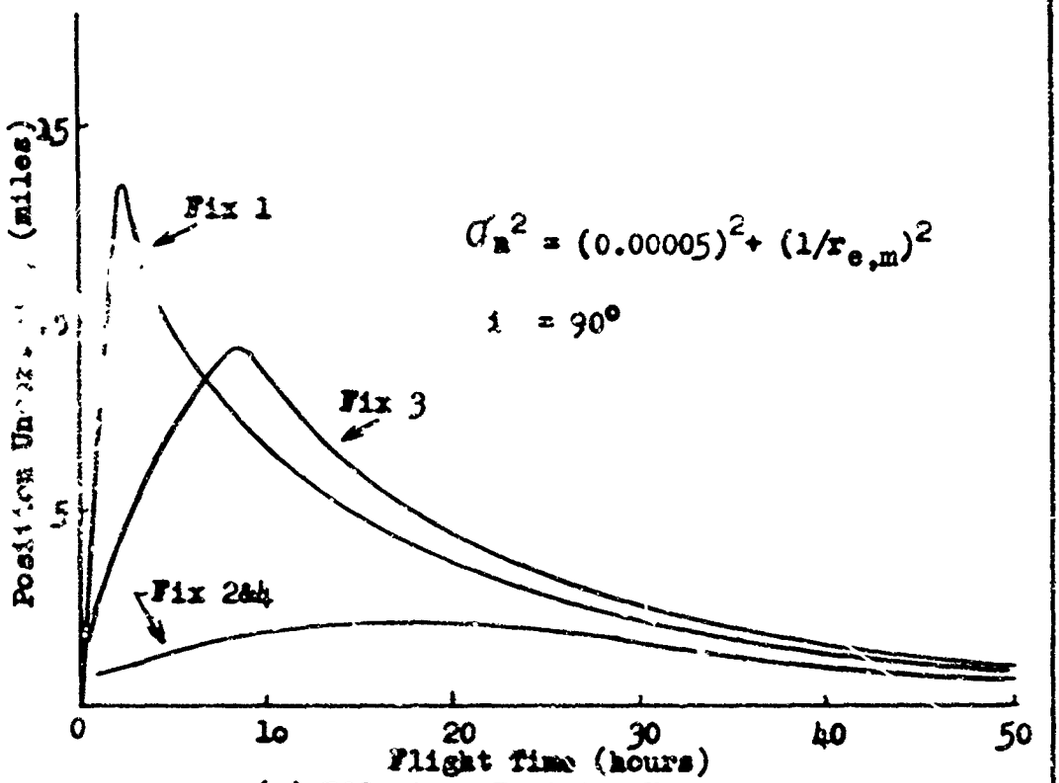

(a) Effect on Position Uncertainty

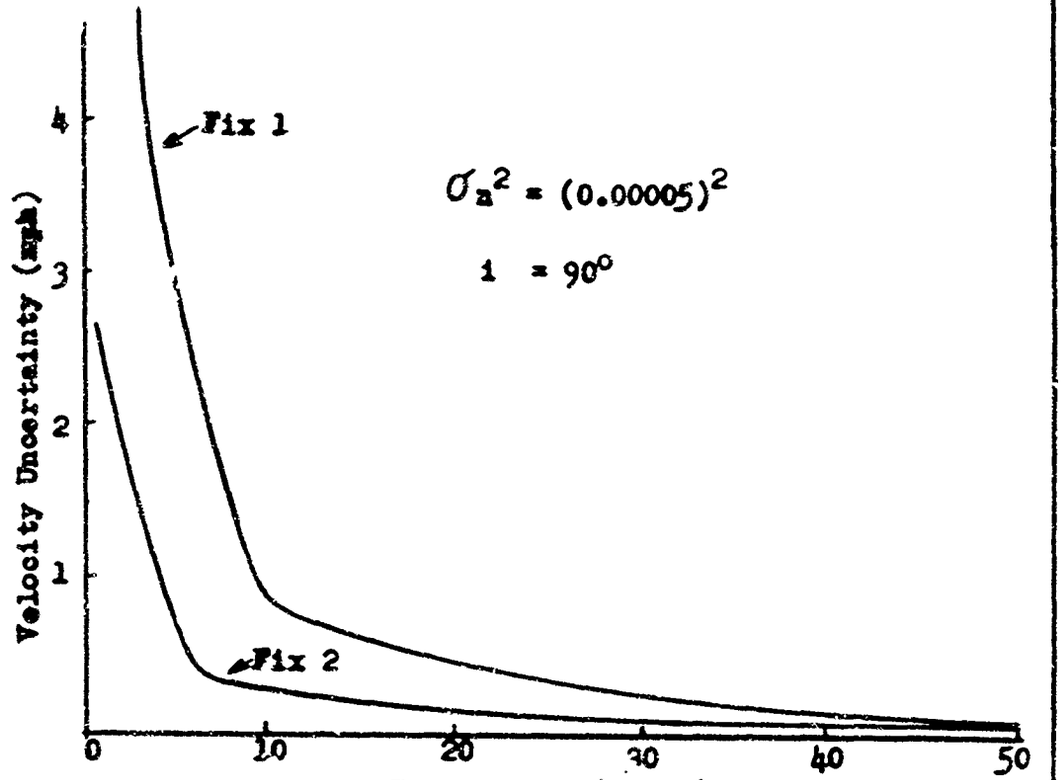

(b) Effect on Velocity Uncertainty

Fig 1. The Effect of Navigation Measurements on Uncertainty in Position and Velocity. (Δt_Y = 30 min)

Table I

The Effect of Navigational Measurements on Uncertainty in Position and Velocity

Note: This data is taken from the same computer results used to plot Fig. 1.

Nav. Fix	Position Uncertainty (mi.)			Velocity Uncertainty (mph)		
	Maximum	Mid.	Final	Maximum	Mid.	Final
1	13.667 (2.5)[a]	2.841	.951	9.829 (1.)[a]	.1411	.0189
2	2.092 (14.)[a]	1.930	.787	5.161 (.5)[a]	.0959	.0152
3	9.321 (9.0)[a]	3.222	.972	____[b]	____[b]	____[b]
4	2.081 (16.)[a]	1.930	.787	____[b]	____[b]	____[b]

a Time in hours after time of launch when maximum occured.

b No data taken.

Table II

The Effect of the Inclination of the Lunar and Spacecraft Planes on the Uncertainty in Position and Velocity

Note: This data is taken from the same computer results used to plot Fig. 2.

Inclin. Angle (degrees)	Position Uncertainty (mi)			Velocity Uncertainty (mph)		
	Maximum	Mid.	Final	Maximum	Mid.	Final
0	56.610 (14.8)[a]	13.946	2.331	15.349 (.25)[a]	.7609	.0597
30	15.264 (1.5)[a]	10.677	4.075	17.057 (.25)[a]	.5137	.0539
60	39.166 (4.8)[a]	3.450	1.306	15.830 (.25)[a]	.1809	.0243
90	5.693 (4.3)[a]	1.916	0.665	16.126 (.25)[a]	.1008	.0135

a See Table I.

As expected Fix 1 has the largest uncertainty in position (13.667 miles) since it uses only earth-moon angular measurements, but the curve for Fix 3 which also considers apparent earth-moon diameter measurements crosses and remains above the former curve after 7.5 hours of flight. Because of these results, the earth and moon diameter measurements are not considered in the remaining sections of this chapter.

All final position uncertainty values are below one mile. The velocity uncertainty curve for Fix 1 remains above the curve for Fix 2 for all flight times and the Fix 1 curve reaches a maximum of 9.829 mph, compared to a maximum of 5.160 mph for Fix 2. Both final velocity uncertainty values fall below 0.025 mph.

Effect of Inclination

The effect of the use of coplanar and non-coplanar trajectories on position and velocity uncertainties using Fix 1 is shown in Fig. 2 and Table II. Inclination angles of 0°, 30°, 60°, and 90° are considered. The time spacing between each navigation fix is held constant at 15 minutes and a constant variance in the errors of the measuring device is assumed. Curves for Fix 2 and a non-coplanar reference trajectory are also shown for comparison purposes.

The coplanar trajectory resulted in the highest maximum value for the uncertainty in position (56.610 miles) but the curve drops below the curve corresponding to an inclination angle of 30° after 30.25 hours of flight. For an inclination angle of 90°, the position uncertainty curve reaches a maximum value of only 5.693 miles and it

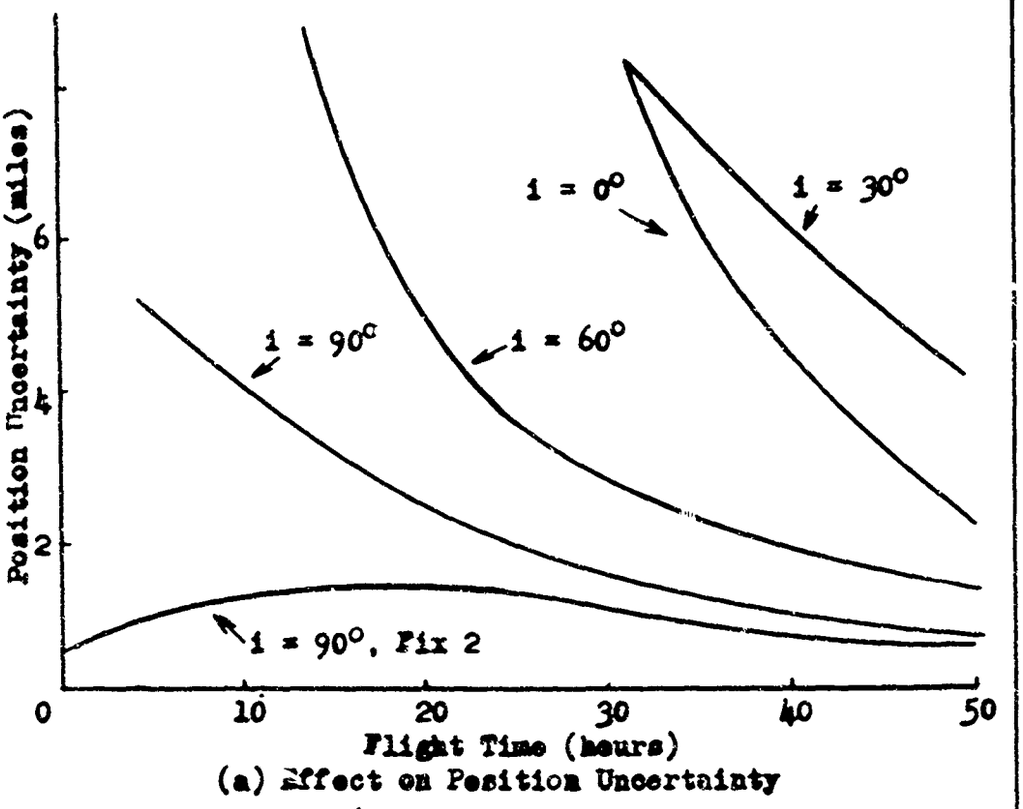

(a) Effect on Position Uncertainty

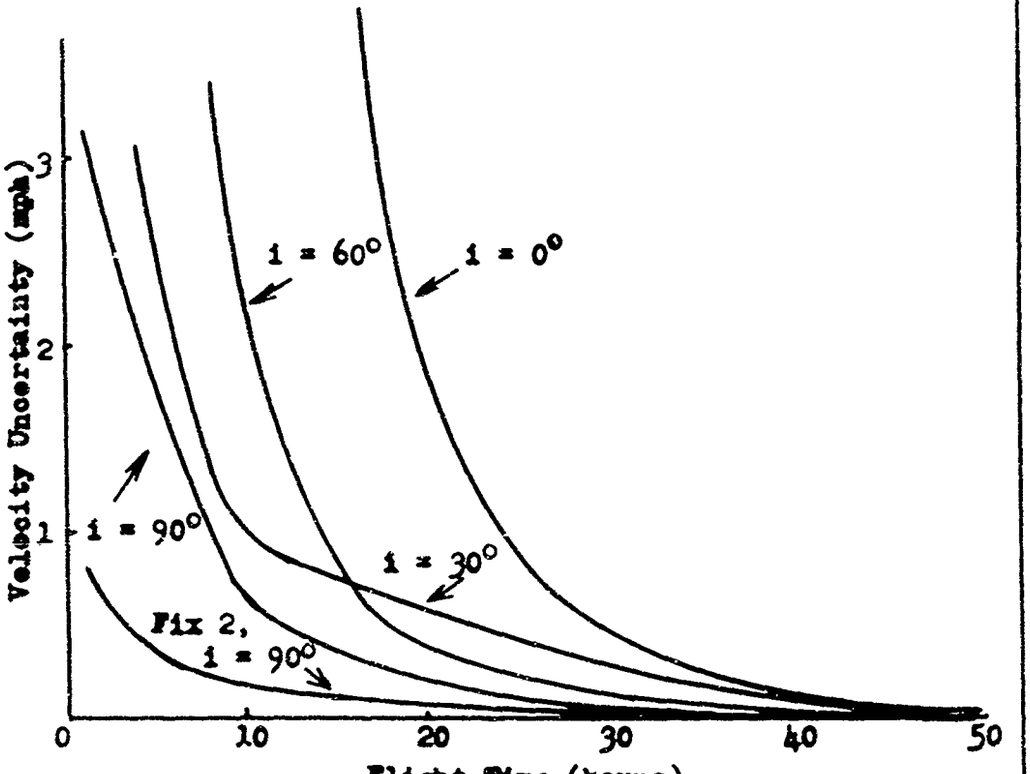

(b) Effect on Velocity Uncertainty

Fig 2. The Effect of Inclination of the Lunar and Reference Trajectory Planes on Uncertainty in Position and Velocity. (Fix 1, Δt_f = 15 min, $\sigma n^2 = (0.00005)^2$)

is the only curve to drop below one mile. The maximum velocity uncertainties compare in order of magnitude for all values of inclination angles considered but the curve for 90° drops much faster than the others. The curve for all inclination angle of 30° crosses above the curve for 60° after 14.50 hours of flight. Only the final velocity uncertainties for inclination angles of 60° and 90° are below 0.025 mph.

Effect of Fix Spacing

The effect on position and velocity uncertainties by using different time spacings between each navigation fix is shown in Fig. 3 and Table III. These values are for Fix 1 using an inclination angle of 90° and assuming a constant variance in the errors of the optical measuring device. Curves and data are shown for fix time intervals of one hour, 30 minutes, 15 minutes, 5 minutes, and one minute.

From the curves it can be seen that the shorter the time spacing between each navigation fix, the lower the uncertainties in both position and velocity. For a time spacing between each fix of one minute, the maximum uncertainty in position is only 0.430 miles as compared to 12.34 miles for a one hour time spacing. Only the curves for time intervals of one and five minutes fall below a final value of one mile. In general the velocity uncertainty curves follow the same pattern as the position curves, although their maximum values do not. The maximum velocity uncertainty of 16.126 mph occurs on the curve for a fix spacing of 15 minutes and the smallest maximum of

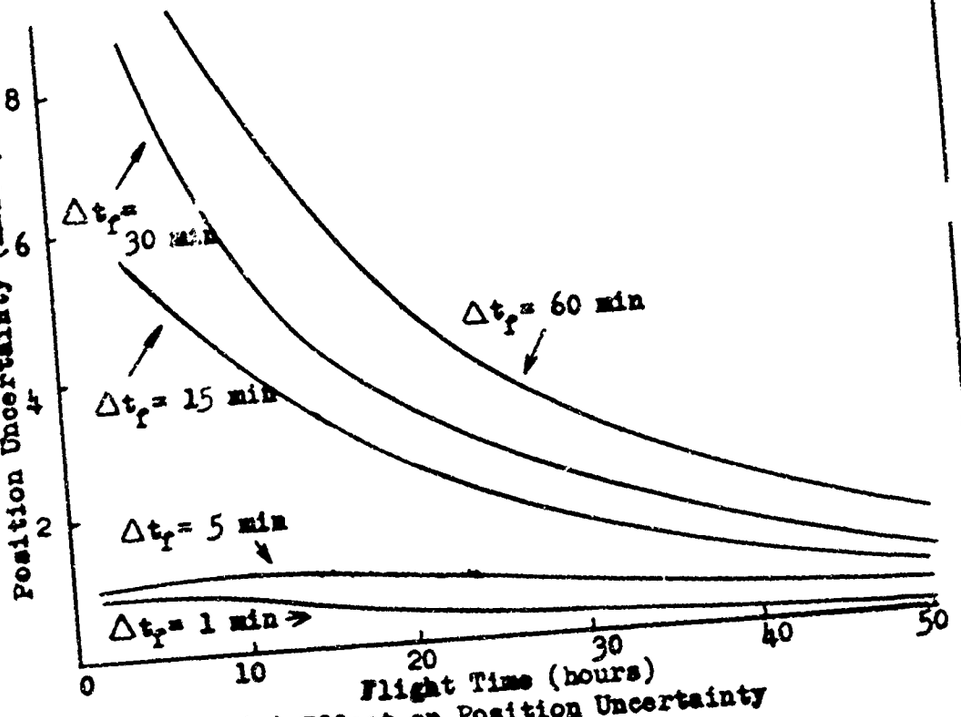

(a) Effect on Position Uncertainty

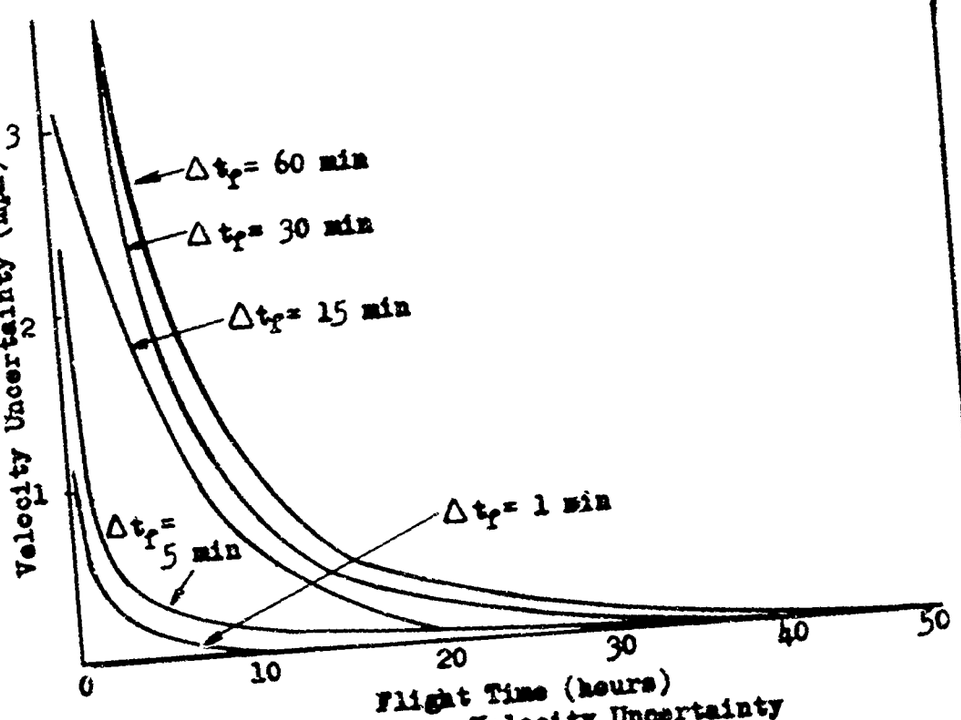

(b) Effect on Velocity Uncertainty

Fig. 3. The Effect of Spacing on the Uncertainty in Position and Velocity. (Fix 1, $i=90^{\circ}$, $\sigma n^2 = (0.00005)^2$)

Table III

The Effect of Fix Spacing on the Uncertainty in Position and Velocity

Note: This data is taken from the same computer results used to plot Fig. 3.

Δt_f (Hours)	Position Uncertainty (mi.)			Velocity Uncertainty (mph)		
	Maximum	Mid.	Final	Maximum	Mid.	Final
1	12.337 (3.0)[a]	3.709	1.295	9.892 (1.0)[a]	.1946	.0260
½	11.392 (2.0)[a]	2.686	.932	9.829 (1.0)[a]	.1411	.0189
¼	5.693 (4.3)[a]	1.916	.665	16.126 (.25)[a]	.1008	.0135
1/12	1.681 (.17)[a]	0.864	.366	12.527 (.17)[a]	.0454	.0075
1/60	0.430 (4.4)[a]	0.203	.054	11.363 (.02)[a]	.0109	.0014

a See Table I

Table IV

The Effect of Sextant Error on the Uncertainty in Position and Velocity

Note: This data is taken from the same computer results used to plot Fig. 4.

Sextant Error[b]	Position Uncertainty (mi.)			Velocity Uncertainty (mph)		
	Maximum	Mid.	Final	Maximum	Mid.	Final
σn_a^2	9.304 (2.8)[a]	2.032	.678	16.430 (.25)[a]	.1067	.0137
σn_b^2	6.873 (2.8)[a]	1.437	.480	16.272 (.25)[a]	.0755	.0097
σn_c^2	5.693 (4.3)[a]	1.916	.665	16.126 (.25)[a]	.1008	.0135
σn_d^2	4.050 (4.0)[a]	1.355	.470	16.095 (.25)[a]	.0713	.0096

a See Table I

b σn_a^2 is defined by Eq. D-2 in Appendix D, $\sigma n_b^2 = \frac{1}{2}\sigma n_a^2$

$\sigma n_c^2 = (0.00005)^2$ rad., $\sigma n_d^2 = \frac{1}{2}\sigma n_c^2$

9.829 mph occurs on the curve for a spacing of 30 minutes. All final velocity uncertainties are below 0.025 mph except for the curve for a one hour fix spacing.

Effect of Sextant Errors

The effect of using different values for the variance in the errors of the optical measuring device on uncertainty in position and velocity is shown in Fig. 4 and Table IV using Fix 1. The time interval between each fix is held constant at 15 minutes and the reference trajectory plane is inclined to the lunar plane at 90^{o}. Four different values for the variance are considered (Table IV, Note b).

As expected, the maximum uncertainty in position of 9.304 miles occurs on the curve related to σn_a^2, as this curve accounts for the larger uncertainty in defining the horizon when the vehicle is near the earth or moon. The maximum position uncertainty for the constant variance σn_c^2 is 5.693 miles. After about 25 hours of flight, the curves corresponding to σn_a^2 and σn_c^2 are almost identical as are the curves for σn_b^2 and σn_c^2. All position uncertainties at arrival are less than one mile and the velocity uncertainty curves follow a pattern similar to the position curves. The maximum velocity uncertainty occurs on the curve for σn_a^2 at 16.430 mph and the minimum is on the curve for σn_d^2 at a value of 16.095 mph. All final velocity uncertainties are less than 0.025 mph.

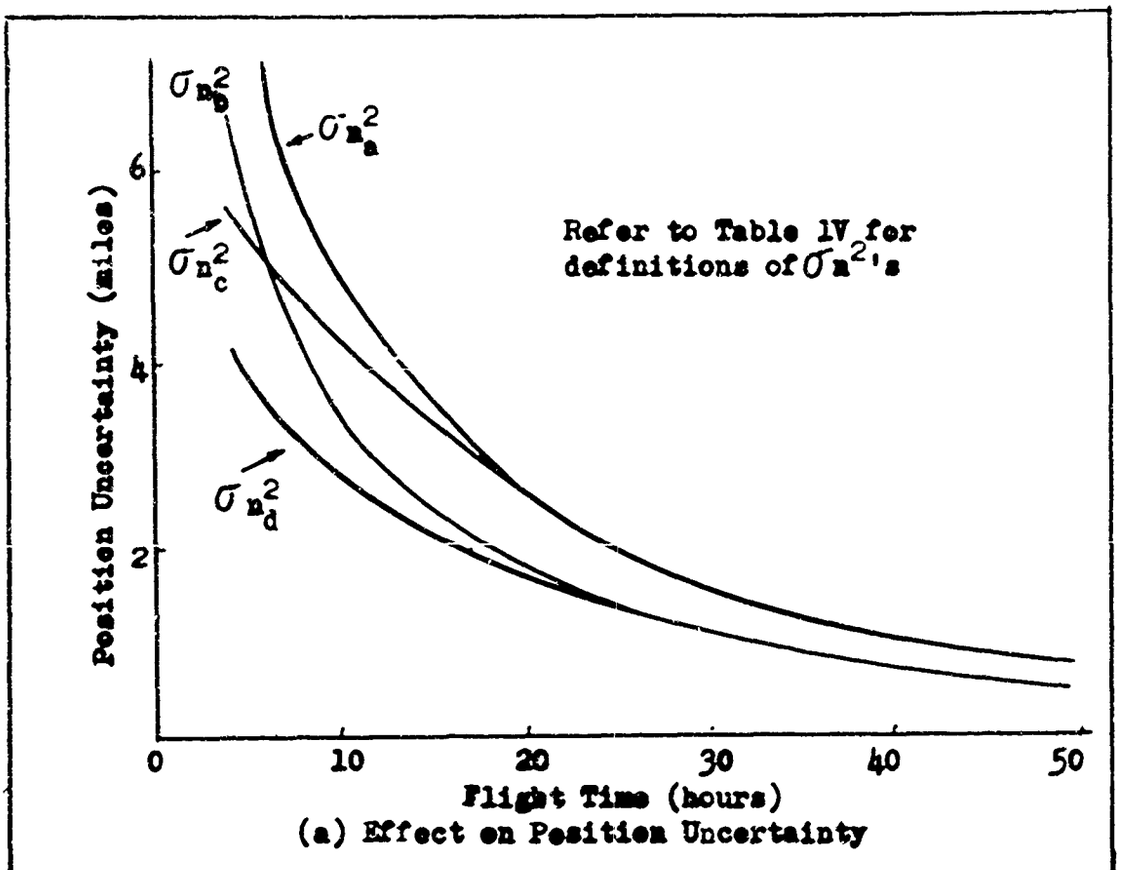

(a) Effect on Position Uncertainty

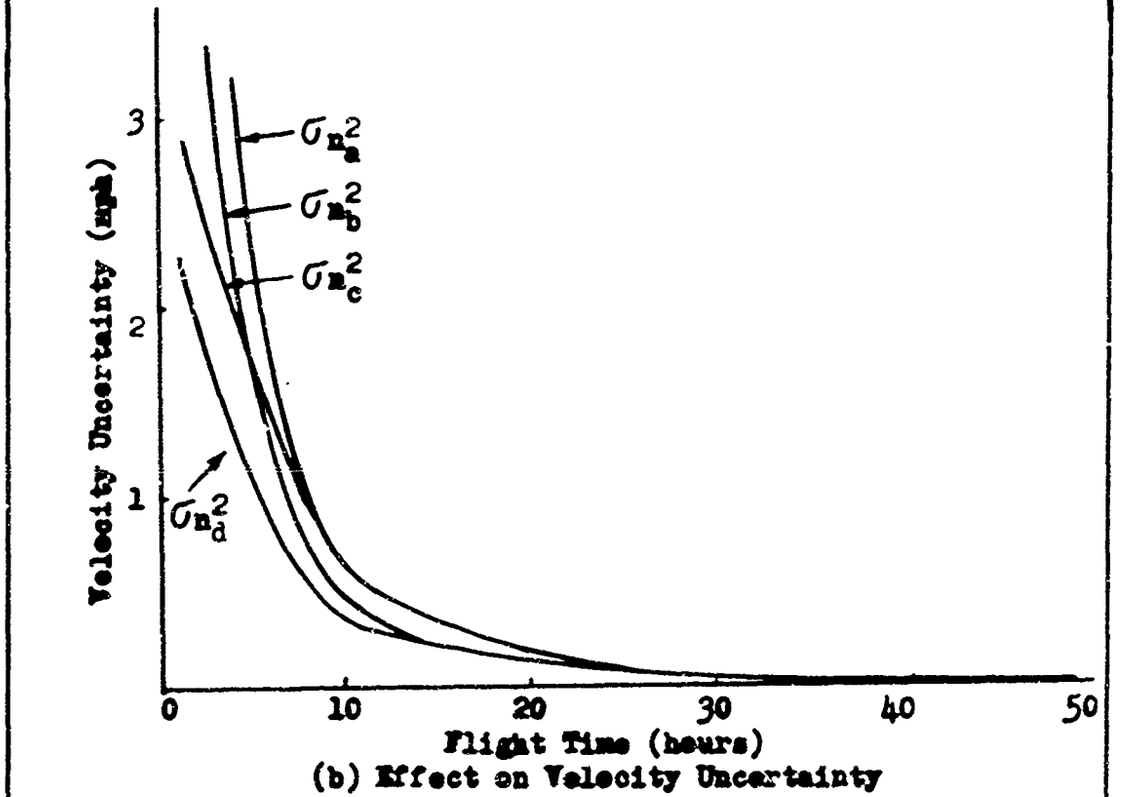

(b) Effect on Velocity Uncertainty

Fig. 4. The Effect of Sextant Errors on the Uncertainty in Position and Velocity. (Fix 1, $i=90^\circ$, $\Delta t_f = 15$ min)

Comparison of Fix 1 and Fix 2

Fig. 5 and Table V show a coplanar comparison between Fix 1 and Fix 2. Fix 2, with a time spacing between each measurement held constant at 15 minutes, is considered the standard. Each fix uses σn_a^2 as the variance in the errors of the optical measuring device. Fix 1 is plotted for constant fix spacings of one minute and 30 seconds respectively. The former curve has a maximum position uncertainty of 14.634 miles and the latter 10.095 miles as compared to 7.011 miles for Fix 2. Both position uncertainty curves for Fix 1 drop below the curve for Fix 2 before 40 hours of flight and all final position uncertainties are less than one mile. Fix 1, with a time spacing between each fix of 1 minute, has a maximum velocity uncertainty of 12.878 mph and the same Fix, with a time spacing between each fix of 30 seconds, has a maximum velocity uncertainty of 12.614 mph as compared to 14.953 mph for Fix 2. Both velocity uncertainty curves for Fix 1 exhibit a plateau region between times of flight of approximately 3 to 15 hours which are probably the result of the non-optimum nature of the earth-moon angular measurements during the early part of the flight. All final velocity uncertainties are less than 0.025 mph.

Fig. 6 and Table VI show a non-coplanar comparison between Fix 1 and Fix 2. The inclination angle is 90° and the same variance in the errors of the optical measuring device is assumed as used above. The time spacing for Fix 2 is again 15 minutes and Fix 1 is plotted for time spacings of five and one minutes. The maximum position uncertainty for Fix 1, with a time spacing between measurements

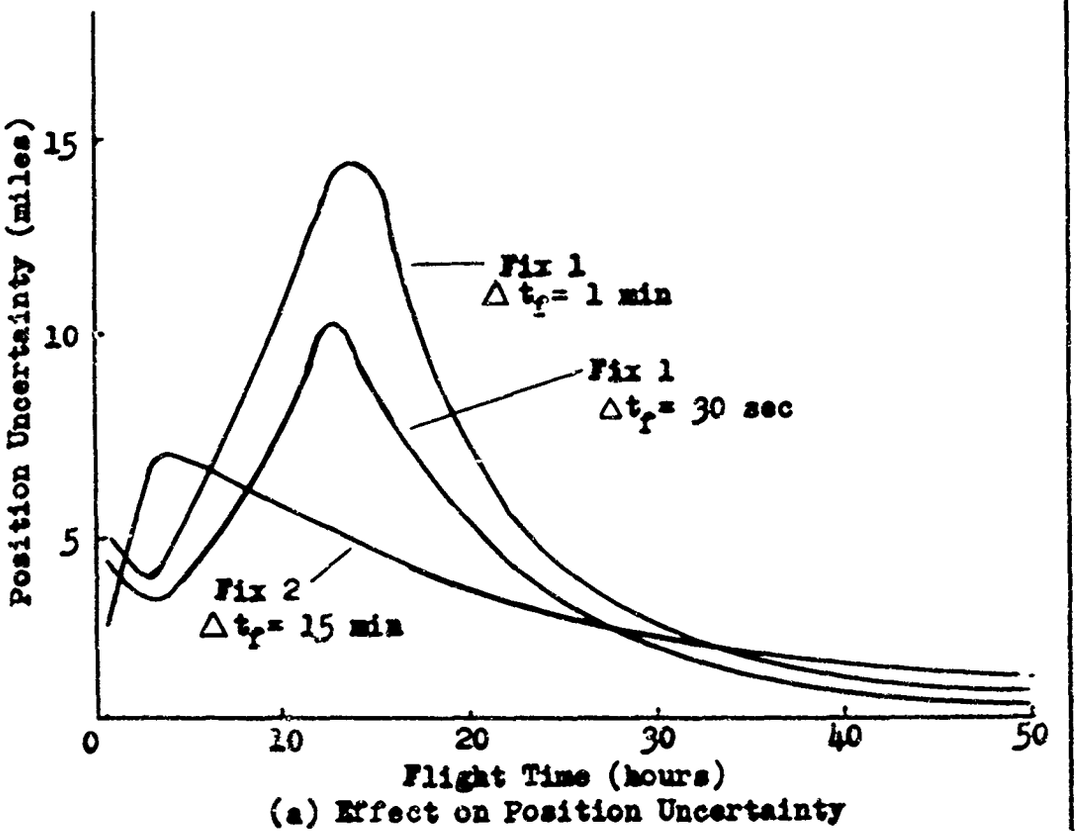

(a) Effect on Position Uncertainty

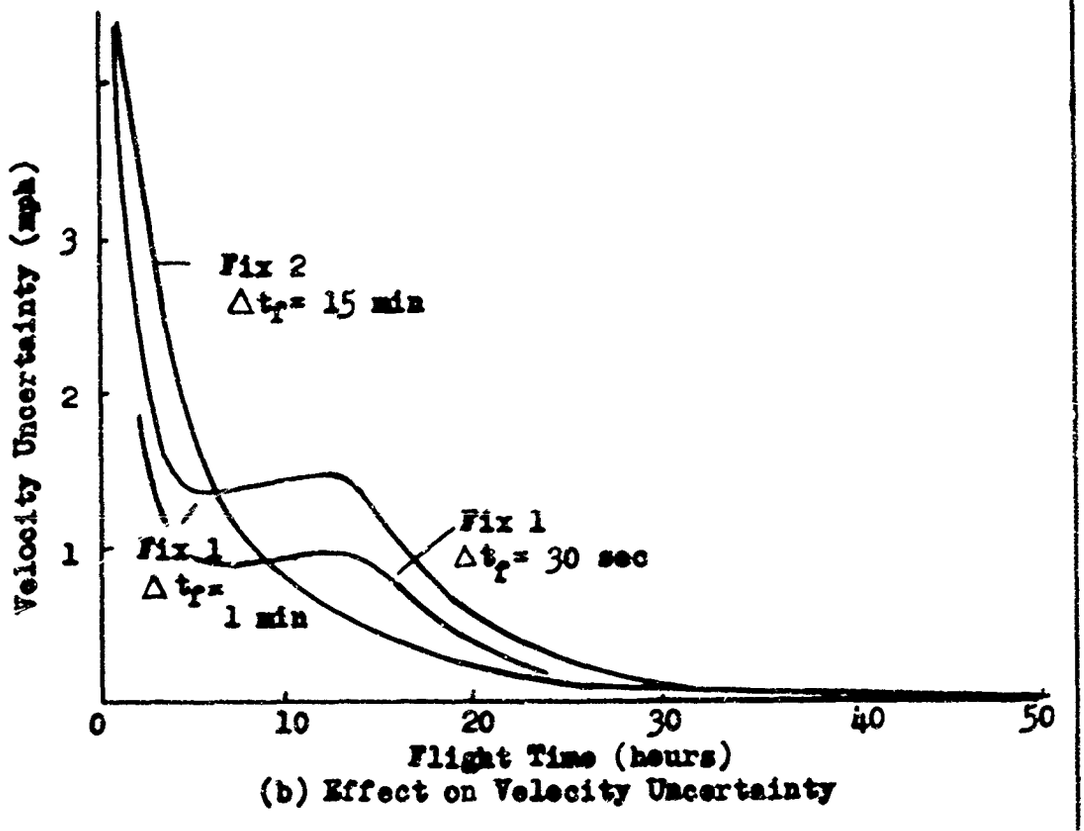

(b) Effect on Velocity Uncertainty

Fig. 5. Coplanar Comparison of Fix 1 and Fix 2. ($i=0^{\circ}$, σn_a^2)

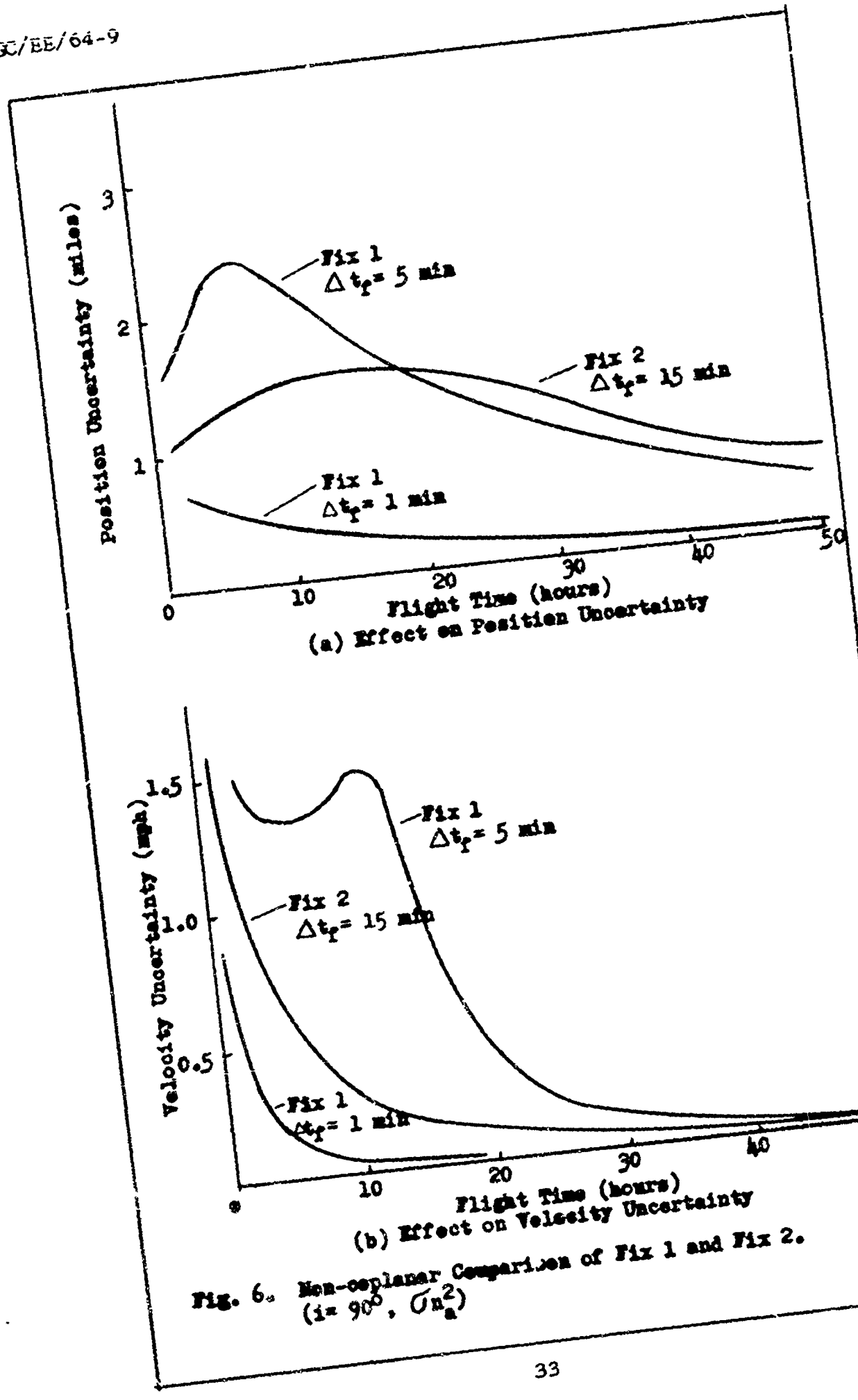

Fig. 6. Non-coplanar Comparison of Fix 1 and Fix 2. ($i = 90^\circ$, $\sigma_{n_a}^2$)

Table V
Coplanar Comparison of Fix 1 and Fix 2 ($i = 0^{\circ}$)

Note: This data is taken from the same computer results used to plot Fig. 5.

Nav. Fix	Position Uncertainty (mi)			Velocity Uncertainty (mph)		
	Maximum	Mid	Final	Maximum	Mid	Final
1[b]	14.634 (13.8)[a]	3.735	0.620	12.878 (0.18)[a]	0.2038	0.0159
1[d]	10.095 (11.9)[a]	2.640	0.438	12.614 (0.15)[a]	0.1440	0.0112
2[c]	7.011 (3.75)[a]	2.333	0.788	14.953 (0.25)[a]	0.1260	0.0200

a See Table I

b $\Delta t_f = 1$ min

c $\Delta t_f = 15$ min

d $\Delta t_f = 30$ sec

Table VI
Non-coplanar Comparison of Fix 1 and Fix 2 ($i = 90^{\circ}$)

Note: This data is taken from the same computer results used to plot Fig. 6.

Nav. Fix	Position Uncertainty (mi)			Velocity Uncertainty (mph)		
	Maximum	Mid	Final	Maximum	Mid	Final
1[b]	2.409 (7.08)[a]	1.148	0.392	12.655 (0.17)[a]	0.0604	0.0080
1[d]	1.302 (0.32)[a]	0.216	0.079	11.364 (0.02)[a]	0.0116	0.0018
2[c]	1.507 (12.7)[a]	1.382	0.559	6.923 (0.25)[a]	0.0693	0.0108

a See Table I

b $\Delta t_f = 5$ min

c $\Delta t_f = 15$ min

d $\Delta t_f = 1$ min

of five minutes, is 2.409 miles and the maximum for the same Fix, with a time spacing of one minute, is 1.302 miles as compared to 1.507 miles for Fix 2. All final position uncertainties are less than one mile. The maximum velocity uncertainties for Fix 1 are 12.655 mph and 11.3638 mph as compared to 6.9226 mph for Fix 2. The velocity uncertainty curve for Fix 1, with a time spacing of five minutes, shows a plateau region early in the flight as was found with the coplanar curves. All final velocity uncertainties are less than 0.025 mph.

V. Conclusions

The requirement for estimating the position and velocity accurately along an earth-moon freefall trajectory using only earth-moon angular measurements and an on-board computer capable of computing the recursive navigation equations has been met. As shown in the preceding section, updating the navigation information every minute or less for the coplanar reference trajectory and every five minutes or less for the non-coplanar reference trajectory will result in acceptable uncertainties in the estimate of position and velocity.

With the use of non-coplanar reference trajectories, a trade-off should be obtainable between the capability of the on-board computer and the desired uncertainties in position and velocity measurements. This study has shown that the use of only earth-moon angular measurements with an on-board recursive navigation system is a feasible navigation technique for a lunar mission.

VI. Recommendations

Various extensions to this study are suggested by Dr. Battin's work as outlined in references 2 and 3. However, the next logical development of this study would be the estimation of velocity correction along the flight path needed to reach the target point (Ref 2:21-36). In this extended study, full use could be made of the perturbation matrices, state transition matrices, and position and velocity estimates generated for this study. The digital programs used in this study can be obtained from Mr. Poole of the A.S.D. Digital Computation Division (see Preface) under problem number 64024 and task number 040A-77137. It is suggested that any new studies be based on the data for Δt_f = 5 min. or less, inclination = 60° or 90°, and $\sigma_n^2 = (0.00005)^2$.

Bibliography

1. Battin, R.H. A Recoverable Interplanetary Space Probe, Volume IV. Report R-235. Cambridge, Mass: M.I.T. Instrumentation Laboratory, July 1959

2. Battin, R.H. A Statistical Optimizing Navigation Procedure for Space Flight. Report R-341. Cambridge Mass: M.I.T. Instrumentation Laboratory, September 1961 (Revised May 1962).

3. Battin, R.H. Astronautical Guidance. New York: McGraw-Hill Book Co., 1964.

4. Buchheim, R.W. Motion of a Small Body in Earth-Moon Space. Rand Research Memo., RM-1726. Santa Monica, California: The Rand Corporation, June 1956.

5. Danby, J.M.A. "Matrix Methods in the Calculation and Analysis of Orbits." A.I.A.A. Journal, 2: 13-16 (January 1964).

6. Duncan, Donald B. "Inertial Guidance and Space Navigation." Journal of the Institute of Navigation, 6: 30-33, (Spring 1958).

7. Frimtzis, R. Lunar Vehicle Guidance Study. Technical Documentary Report ASD-TDR-62-207 San Diego, California General Dynamics/Astronautics, March 1962.

8. Hamer H.A. and A.P. Mayo. Error Analysis of Several Methods of Determining Vehicle Position in Earth-Moon Space from Simultaneous Onboard Optical Measurements. NASA Report TN D-1805. Hampton, Va: Langley Research Center, June 1963.

9. Harter, G.A. Error Analysis and Performance Optimization of Rocket Vehicle Guidance Systems, Chapter 12, Inertial Guidance Edited by G.R. Pitman. New York: John Wiley and Sons Inc., 1962.

10. Huss, C.R. H.A. Hamer, and J.P. Mayer. Parameter Study on Insertion Conditions for Lunar Missions Including Various Trajectory Considerations. NASA Report TR R-122. Langley AFB, Va: Langley Research Center, 1961.

11. Jones, R.L. and A.P. Mayo. A Study of Some Transition Matrix Assumptions in Circumlunar Navigation Theory. NASA Report TN D-1812. Hampton, Va: Langley Research Center, October 1963.

12. Kalman, R.E. "A New Approach to Linear Filtering and Prediction Problems." Transactions of the A.S.M.E., Series D. 82: 35-45, (March 1960).

13. Michael, W.H. Jr. and R.H. Tolson. Effect of Eccentricity of the Lunar Orbit, Oblateness of the Earth, and Solar Gravitational Field on Lunar Trajectories. NASA Report TN D-227. Langley Field, Va: Langley Research Center, June 1960.

14. Schwaniger, A J. Trajectories in the Earth-Moon Space with Symmetrical Free Return Properties. NASA Report TN D-1833. Huntsville, Ala: George C. Marshall Space Flight Center, June 1962.

15. Scott, D.R., C.J. Januska, and R.E. Willes. Optimum Statistical Operations with Celestial Fix Data for Interplanetary Navigation. Unpublished M.S. Thesis (T-298). Massachusetts Institute of Technology, June 1962.

16. Swanlund, George, "Analysis Techniques to Determine Guidance Computation Requirements for Space Vehicles." American Rocket Society Journal, 32: 755-761 (May 1962).

Appendix A

Lunar Reference Trajectory

The utilization of trajectory shapes which bring an exploring vehicle from the earth to a point arbritrarily near the moon and, which if allowed to continue, return the lunar vehicle to the earth with such conditions that reentry and recovery are feasible, might be attractive for both instrumented and manned flights. Photographing the surface of the moon, determination of astronomical constants by observation of trajectory perturbation, and checkout of hardware are examples of unmanned lunar missions. The first manned exploration flights may be "free-return" circumlunar flights with no plan to land on the moon. If the manned mission is to land on the moon, a "free-return" trajectory may be used so that if difficulties arise which would make the lunar landing undesirable the astronauts will return safely to the earth (Ref 14:1-2).

Because this is a feasibility study and to simplify the reference trajectory calculations, several simplifying assumptions relating to the mathematical model of the earth-moon system have been made.

(1) The earth and moon are homogenous spheres and are considered point masses.

(2) The earth is located at the center of its sphere of influence and when the lunar vehicle is traveling inside this sphere, its "free-return" trajectory is effected only by the gravitational

field of the earth. Thus during this portion of flight, the path of the spacecraft describes a conic with the earth at one focus which will be elliptic, parabolic, or hyperbolic depending on the insertion parameters. An analogous situation exists after the spaceship enters the sphere of influence of the moon with the exception that the path of the vehicle will always be hyperbolic. The approximate radius of the sphere of influence of the moon has been calculated to be 35,781 miles (Ref 10:29).

(3) The reference trajectory is high enough above the earth that the effects of the atmospheric drag may be neglected.

(4) The moon revolves about the center of the earth in the lunar plane with a circular orbit of 238,857 statute miles (one lunar unit) and at an angular rate of 0.22997084 rad/day (Ref 10:29).

(5) The effects of the sun, planets, meteroids, and other perturbing bodies are neglected.

(6) The effect of the pressure of solar radiation is neglected.

The effects of the neglected factors on the lunar reference trajectory are discussed in the literature and are not presented in this paper (Ref 4:61-74; Ref 11:10-11; Ref 13). Deviations resulting from the introduction of the neglected factors can, for the most part, be compensated for by changes in the injection velocity (Ref 7: 3-5).

The reference trajectory can be calculated from a knowledge of the insertion parameters. To increase the operational flexibility

of the mission, launch with a non-zero flight path angle (the flight path angle is defined as the angle between the local horizontal and the velocity vector) from a parking orbit will be considered. The variable insertion conditions are the radius of the parking orbit, flight-path angle, magnitude of the insertion velocity, and the lunar lead angle. For a 4100 mile parking orbit radius, insertion velocities below the parabolic escape velocity of 36,063 ft/sec will result in elliptical outgoing trajectories. The insertion parameters selected for this study (Table A-1) will result in a coplanar circumlunar mission that will bring the vehicle to within 1000 miles of the surface of the moon and return the spaceship to within 40 miles of the surface of the earth (Ref 8:23). Only the outgoing elliptical portion of the reference trajectory from launch to the moon's sphere of influence is used in this study (Fig A-1) as this portion represents a large percent of the total distance traveled on a lunar mission. The equations for calculation of the elliptical parameters are listed in Reference 10: Appendix B.

Additional mission flexibility can be obtained if non-coplanar reference trajectories are also considered. The lunar plane (x, y) is inclined to the reference trajectory plane (a,b) at various inclination angles to obtain the effect of using non-coplanar reference trajectories. This method of inclining the two planes eliminates the necessity to recompute the state transition matrices. Transformation from the lunar coordinates (x,y,0) to the inertial

Table A.1

Trajectory Insertion Parameters

Insertion Parameter	Symbol	Value	Remarks
Radius of Parking Orbit	R_L	4100 miles	The radius of the intermediate or launch orbit as measured from the center of the earth
Flight-path angle	γ_L	40 degrees	Angle between the local horizon and the velocity vector
Velocity	V_L	35,900 ft/sec	Value chosen is 163 ft/sec less than parabolic escape velocity
Lunar lead angle	τ	57 degrees	Angle between the radius vectors from the center of the earth to the moon and to the launch point at time of launch.

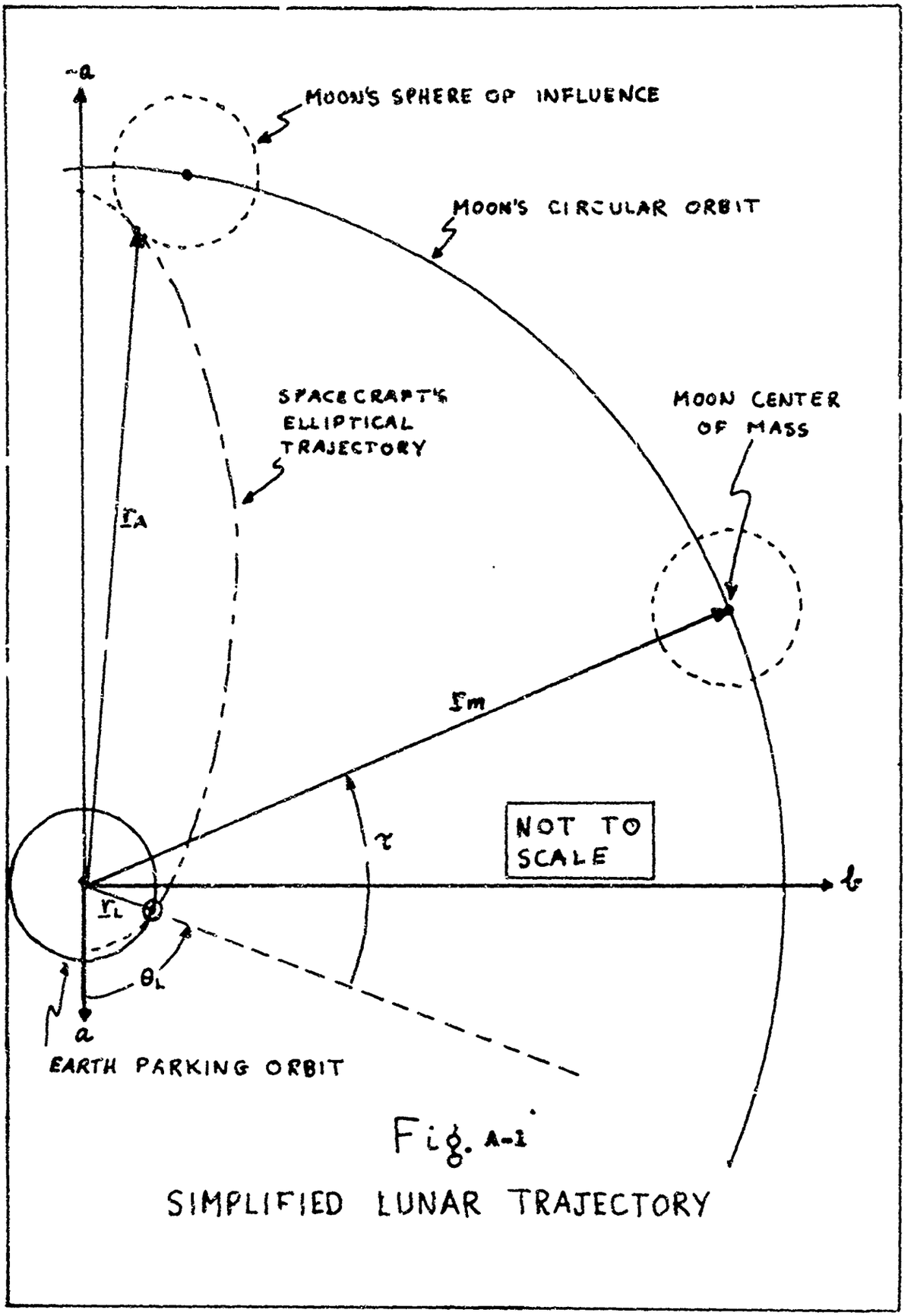

Fig. A-1

SIMPLIFIED LUNAR TRAJECTORY

coordinates (a,b,c), is given by (The inertial coordinate system is defined in Appendix C.)

$$\begin{bmatrix} a \\ b \\ c \end{bmatrix} = M_i \begin{bmatrix} x \\ y \\ 0 \end{bmatrix}$$

where

$$M_i = \begin{bmatrix} 1 & 0 & 0 \\ 0 & \cos i & -\sin i \\ 0 & \sin i & \cos i \end{bmatrix}$$

and i is the inclination angle between the lunar plane and the reference trajectory plane.

Appendix B

Navigational Measurements

The best choice of celestial measurements made at any instant of time along a space trajectory depends on the position of the spacecraft within the geometry of the Space System. In this study a variety of measurements made on different sets of celestial objects in an Earth-Moon System is possible. The problem is to define the possible measurements at each instant of time and determine which measurement yields the best estimate in position as defined by Eq (34) in Section III.

It is assumed in this analysis that the spacecraft clock is perfect. This assumption is consistent with the accuracy of present day spacecraft clocks on comparatively short space trajectories, such as the 50 hour lunar trajectory considered in this study. In addition, the time interval required to make a single celestial measurement can be neglected, since the measuring device can be programmed to search out and hold the selected celestial objects prior to the time of measurement. The relationship between position error and measurement error is essentially linear over a relatively wide range. Therefore, a linear perturbation theory can be used for detailed studies of any of the methods discussed in this appendix (Ref 8:12).

It was stated in Section II that each measurement establishes a component of spacecraft position along some direction in space. If Q is the quantity to be measured and δQ is the difference between

the true and the reference values, then it can be shown that the deviation in spacecraft position $\delta \underline{r}$ is

$$\delta Q = \underline{h}^T \hat{\delta} \underline{r} \qquad \text{(B-1)}$$

regardless of the type of measurement (Ref 3:223-225). Thus, the h vector alone will characterize the type of measurement.

In the interest of computing simplicity, the celestial objects used in this study were the earth, moon, and six (6) stars arbitrarily located at an infinite distance along the coordinate axes of the space coordinate system.

Earth-Moon Measurement

It can be shown (Ref 3:223-225) that for the earth-moon measurement

$$\underline{h} = \frac{\underline{n}_1 - (\underline{n}_1 \cdot \underline{n}_2)\underline{n}_2}{r \sin A} + \frac{\underline{n}_2 - (\underline{n}_1 \cdot \underline{n}_2)\underline{n}_1}{\bar{z} \sin A} \qquad \text{(B-2)}$$

where $\underline{n}_1$ and $\underline{n}_2$ are the unit vectors from a point on the reference trajectory to the earth and moon centers respectively, r and $\bar{z}$ are the distances from the reference point to the earth and moon centers respectively, and A is the angle from the earth line to the moon line.

Planet-Star Measurement

This is simply a special case of the earth-moon measurement. Eq B-2 can be modified to express the geometry vector of the earth-star measurement as follows:

$$\underline{h} = \frac{\underline{n}_s - (\underline{n}_1 \cdot \underline{n}_s)\,\underline{n}_1}{r \sin A_E} \qquad \text{(B-3)}$$

where $\underline{n}_s$ is the unit vector from a point on the reference trajectory to the star and A_E is the angle from the earth line to the star line.

Likewise, a similar relationship can be formulated for a moon-star measurement.

$$\underline{h} = \frac{\underline{n}_s - (\underline{n}_2 \cdot \underline{n}_s)\,\underline{n}_2}{Z \sin A_M} \qquad \text{(B-4)}$$

where, A_M is the angle from the moon line to the star line.

Apparent Diameter of a Planet Measurement

The geometry vector for the apparent diameter of a planet (Ref 3:223-225) can be computed by

$$\underline{h} = \frac{2\, d_p\, \underline{n}_p}{x(4\,x^2 - d_p^2)^{1/2}} \qquad \text{(B-5)}$$

where d_p is the actual diameter of the planet ($d_E = 41.78127 \times 10^6$ ft. and $d_M = 11.40573 \times 10^6$ ft), x is the distance from the point on the reference trajectory to the planet center (r for the earth and Z for the moon), and $\underline{n}_p$ is the unit vector from reference point to the planet center ($\underline{n}_1$ for the earth and $\underline{n}_2$ for the moon).

Appendix C

The Fundamental Perturbation Matrices

The procedure used to generate the perturbation matrices discussed in Section II is developed in outline form in Reference 1: pgs. 761-773. Since the perturbation matrices in this study were developed for the elliptical spacecraft reference trajectory and lunar orbit in the same plane, simplifications to the equation given in the cited reference were made. These simplifications are based on the fact that in this coplanar case,

$$\Omega = -w \tag{C-1}$$

and

$$i = 0 \tag{C-2}$$

As shown in Fig C-1, Ω is the true anomaly of the spacecraft reference trajectory at the time of launch and i is the inclination of the spacecraft reference trajectory and lunar orbit planes measured at the ascending node (AN). The parameter w is defined for the coordinate systems used in the cited reference and has no meaning in the coordinate system of Fig. 1C. It is only stated here as a key to the simplication process.

Computation of R(t) and V(t) Matrices

The equations used to compute the R(t) and V(t) matrices of this study are lised here for reference. The parameters used in these equations are defined in Table C-I. The R(t) and V(t) matrices were written in the form

$$\begin{aligned} R(t) &= R'(t)\ Mpp^T \\ V(t) &= V'(t)\ Mpp^T \end{aligned} \tag{C-3}$$

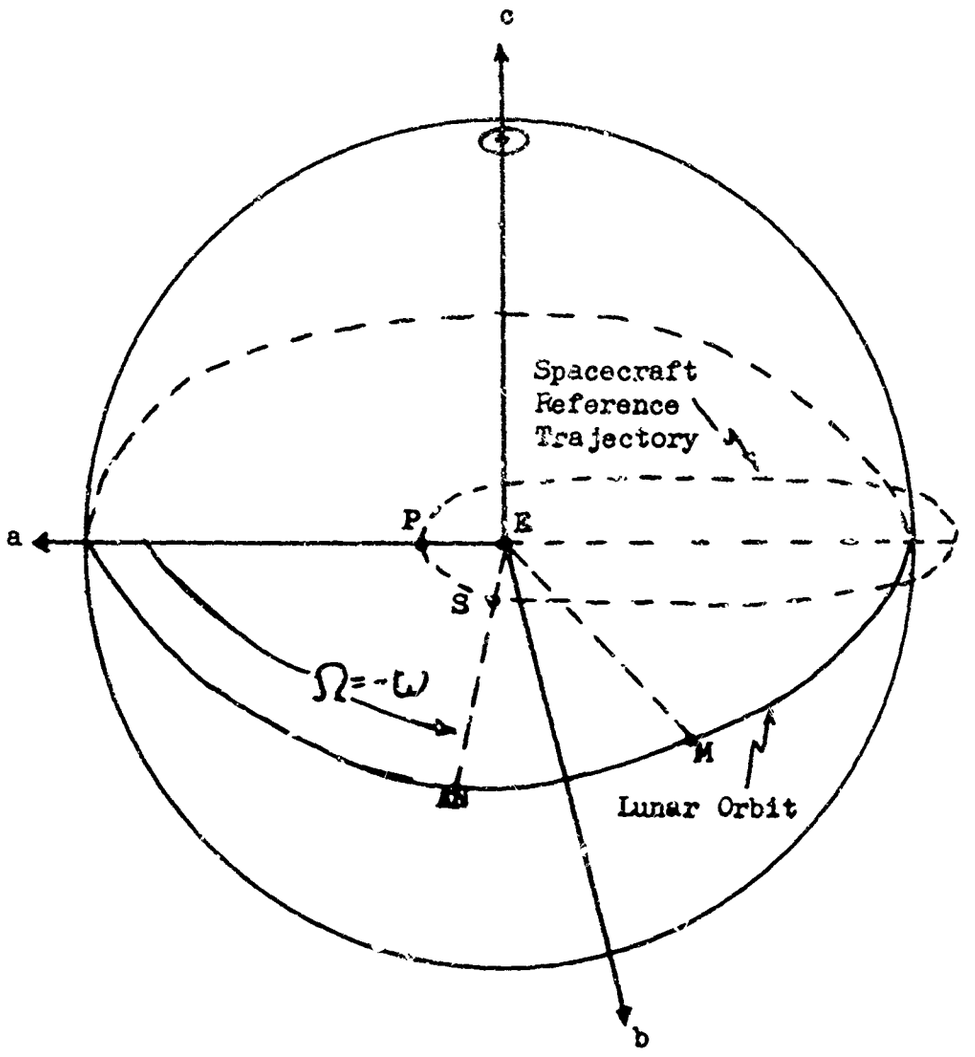

E - Earth center of mass (fixed)

P - Perigee of spacecraft reference trajectory

S - Spacecraft position at launch

M - Moon center of mass at launch

AN - Ascending node for general non-coplanar case outlined in reference 1

Fig. C-1 Space Coordinate System

Table C-I

Reference Trajectory Parameters

Parameter(s)	Definition[1]
t_f	time of flight = t - t_L
t	time measured from perigee
t_L	time of launch measured from perigee (0.0065147892 days)
$r_{(L)}$	position of spacecraft at time t_L (see Fig C-1)
r	position of spacecraft at time t (see Fig C-1)
v	velocity of spacecraft at time t
a	semi-major axis (0.95190686 lunar units[2])
p	semi-latus rectum (0.019964129 lunar units[2])
e	eccentricity (0.98945804)
E	eccentric anomaly at time t_L (0.12312378 rad.)
Ω	true anomaly at time t_L (1.4052372 rad)
μ	gravitational parameter (0.05386804 l.u.^{3}/day^2)

Note [1] The values listed are computed from equations obtained from Ref i.

[2] 1 lunar unit = 238,857 miles

where

$$Mpp^T = \begin{bmatrix} \frac{r_a(L)}{r(L)} & \frac{r_b(L)}{r(L)} & 0 \\ \frac{-r_b(L)}{r(L)} & \frac{r_a(L)}{r(L)} & 0 \\ 0 & 0 & 1 \end{bmatrix} \tag{C-4}$$

and

$$R'(t) = \begin{bmatrix} R_{11} & R_{21} & 0 \\ R_{12} & R_{22} & 0 \\ 0 & 0 & R_{32} \end{bmatrix} \tag{C-5}$$

$$V'(t) = \begin{bmatrix} V_{11} & V_{21} & 0 \\ V_{12} & V_{22} & 0 \\ 0 & 0 & V_{33} \end{bmatrix}$$

The elements of the $R'(t)$ and $V'(t)$ matrices are as follows:

$$R_{11} = \frac{a\, r_b(L)}{(\mu p)^{\frac{1}{2}}\, r(L)} \left\{ 2e \left[r_a - \frac{3}{2} v_a t_f \right] - \frac{r_b^2}{r} - p - \frac{v_a}{(\mu a)^{\frac{1}{2}}} \sin E \left[2r(L)^2 - \frac{P(P-r(L))}{e^2} \right] \right\} + \frac{(\mu p)^{\frac{1}{2}} r_a(L) r_b}{\mu e\, r(L)} \tag{C-6}$$

$$R_{21} = \frac{(\mu p)^{\frac{1}{2}}}{e\, r(L)} \left\{ 2ae \left[r_a - \frac{3}{2} v_a t_f \right] - \left[\frac{r_b^2}{r} + p \right] \left[a - \frac{r(L)^2}{P} \right] -$$

$$\frac{va}{(\mu a)^{\frac{1}{2}} \sin E}\left[2ar(L)^2 - \frac{P(p-r(L))}{e^2}\left(a - \frac{r(L)^2}{p}\right)\right]\Bigg\} -$$

$$\frac{r_b(L)\ r_b\ (p + r(L))}{(\mu p)^{\frac{1}{2}}\ e\ r(L)} \tag{C-7}$$

$$R_{12} = \frac{a\ r_b(L)}{(\mu p)^{\frac{1}{2}}\ r(L)}\left\{2e\left[r_b - \frac{3}{2}\ v_a\ t_f\right] - \frac{r_a r_b}{r} - \right. \tag{C-8}$$

$$\left.\frac{v_b}{(\mu a)^{\frac{1}{2}} \sin E}\left[2r(L)^2 - \frac{P(p-r(L))}{e^2}\right]\right\} - \frac{(\mu p)^{\frac{1}{2}} r_a(L) r_a}{\mu\ e\ r(L)}$$

$$R_{22} = \frac{(\mu p)^{\frac{1}{2}}}{\mu e\ r(L)}\left\{2ae\left[-_b - \frac{3}{2}\ v_b\ t_f\right] - \left[\frac{r_a r_b}{r}\right]\left[a - \frac{r(L)^2}{p}\right] - \right.$$

$$\left.\frac{vb}{(\mu a)^{\frac{1}{2}} \sin E}\left[2ar(L)^2 - \frac{P(p-r(L))}{e^2}\left(a - \frac{r(L)^2}{p}\right)\right]\right\} + \tag{C-9}$$

$$\frac{r_a r_b(L)\ (p + r(L))}{e\ (\mu p)^{\frac{1}{2}}\ r(L)}$$

$$R_{33} = (\mu p)^{-\frac{1}{2}}\left[r_a(L) r_b - r_a\ r_b(L)\right] \tag{C-10}$$

$$V_{11} = \frac{a\ r_b(L)}{(\mu p)^{\frac{1}{2}}\ r(L)}\left\{2e\left[\frac{3}{2}\mu\ \frac{r_a}{r^3}\ t_f - \frac{va}{2}\right] + \frac{va\ ra\ p}{r^2} - \frac{r_b\ v_b}{r} + \right. \tag{C-11}$$

$$\frac{\mu r_a}{r\,(\mu a)^{\frac{1}{2}} \sin E}\left[2r(L)^2 - \frac{P(p - r(L))}{e^2}\right]\Bigg\} + \frac{(\mu p)^{\frac{1}{2}}\, r_a(L) v_b}{\mu e r(L)}$$

$$V_{21} = \frac{(\mu p)^{\frac{1}{2}}}{\mu e r(L)}\Bigg\{2ae\left[\frac{3}{2}\mu\,\frac{r_a}{r^5}\,t_f - \frac{v_a}{2}\right] + \left[a - \frac{r(L)^2}{p}\right]$$

$$\left[\frac{v_a v_a p}{r^2} - \frac{r_b v_b}{r}\right] + \frac{r_a}{e\, r^3 (\mu a)^{\frac{1}{2}} \sin E}\left[2ar(L)^2 -\right.$$

$$\left.\frac{P}{e^2}\,(p - r(L))\left(a - \frac{r(L)^2}{p}\right)\right]\Bigg\} - \frac{r_b(L) v_b\,(p + r(L))}{(\mu p)^{\frac{1}{2}} e\, r\,(L)} \qquad \text{(C-12)}$$

$$V_{12} = \frac{a\, r_b(L)}{(\mu p)^{\frac{1}{2}}\, r(L)}\Bigg\{2e\left[\frac{3}{2}\,\frac{r_b}{r^3}\,t_f - \frac{V_b}{2}\right] + \frac{v_a v_b p}{r^2} + \frac{r_a v_b}{r} + \qquad \text{(C-13)}$$

$$\frac{r_b}{r\,(\mu a)^{\frac{1}{2}} \sin E}\left[2r(L)^2 - \frac{P(p - r(L)}{e^2}\right]\Bigg\} - \frac{(\mu p)^{\frac{1}{2}} r_a(L) v_a}{\mu e r(L)}$$

$$V_{22} = \frac{(\mu p)^{\frac{1}{2}}}{\mu e r(L)}\Bigg\{2ae\left[\frac{3}{2}\mu\frac{r_b}{r^3}\,t_f - \frac{v6}{2}\right] + \left[a - \frac{r(L)^2}{p}\right]$$

$$\left[\frac{v_a\, r_b p}{r^2} + \frac{r_b\, v_b}{r}\right] + \left[\frac{r_b}{e r^3\,(\mu a)^{\frac{1}{2}} \sin E}\right]$$

$$\left[2ar(L)^2 - \frac{P}{e^2}\,(p - r(L))\,(a - \frac{r(L)^2}{p}\right]\Bigg\} + \frac{r_b(L) v_a (p + r(L))}{e\,(\mu p)^{\frac{1}{2}}\, r(L)} \qquad \text{(C-14}$$

$$V_{33} = (\mu r)^{-\frac{1}{2}}\left[r_a(L) v_b - v_a\, r_b(L)\right] \qquad \text{(C-15)}$$

Computation of R*(t) and V*(t) Matrices

The R*(t) and V*(t) matrices are computed using the same equations derived for R(t) and V(t) if t_L is replaced by t_A (time of arrival) and r(L) is replaced by r(A) (position at t_A).

Appendix D

Assumed System Errors

This appendix contains the assumed r.m.s. injection errors, the initial correlation matrix (E_o) based on these errors, and the assumed variance of our optical measuring device (Ref 2:28-29).

Initial Correlation Matrix (E_o)

The correlation matrix of the injection errors is based on the assumed r.m.s. injection errors contained in Table D-I .

Table D-I

Assumed R.M.S. Injection Errors

	Altitude	Track	Range
Position	10,000 ft	15,000 ft	5,000 ft
Velocity	15 ft/sec	6 ft/sec	4 ft/sec

The correlation matrix below was obtained by a transformation from the altitude, track, and range coordinate system of Table D-I to the (a,b,c) coordinate system defined in Fig. C-1. The basic units of the E_o matrix as shown in Eq. D-1 are lunar units $X\ 10^{-10}$ and lunar units per day $X\ 10^{-7}$.

$$E_0 = \begin{bmatrix} 1.087 & -1.019 & -0.413 & 0 & 0 & 0 \\ -1.019 & 0.957 & 0.388 & 0 & 0 & 0 \\ -0.413 & 0.388 & 0.157 & 0 & 0 & 0 \\ 0 & 0 & 0 & 0.557 & -2.553 & -0.647 \\ 0 & 0 & 0 & -2.553 & 11.692 & 2.963 \\ 0 & 0 & 0 & -0.647 & 2.963 & 0.751 \end{bmatrix} \quad \text{(D-1)}$$

The initial uncertainties in position and velocity are 3.543 miles and 11.374 miles per hour.

Variance(σn^2) of the Optical Sextant

The standard deviation of the optical measuring device (sextant) was assumed to be approximately 0.05 milliradians (10 seconds of arc). However, since all the angular measurements in this study are made relatively close to the earth and moon, an additional factor was introduced in some of the computer runs to accomodate the decrease in accuracy as the spacecraft gets close to a planet. Based on these considerations the sextant when measuring the angle between the earth and moon was assumed to have a random error whose variance

$$\sigma n_a^2 = \begin{cases} (0.00005)^2 + \left(\frac{1}{r(t_n)}\right)^2 \text{ rad}, & \text{if } r(t_n) < S(t_n) \\ (0.00005)^2 + \left(\frac{1}{Z(t_n)}\right)^2 \text{ rad}, & \text{if } r(t_n) > S(t_n) \end{cases} \quad \text{(D-2)}$$

where $r(t_n)$ and $Z(t_n)$ are the distances in miles from the spacecraft to the earth and moon, respectively. For measurements involving only one planet, the appropriate variance was used; for example, the measurement of the angle between the earth and a star would use only the first part of Eq. D-2.